Digital Halftoning via Mixed-Order Weighted $\Sigma\Delta$ Modulation

Felix Krahmer
Dept. of Mathematics & Munich Data Science Institute
Technical University of Munich
and Munich Center for Machine Learning
Garching/Munich, Germany
felix.krahmer@tum.de

Anna Veselovska
Dept. of Mathematics & Munich Data Science Institute
Technical University of Munich
and Munich Center for Machine Learning
Garching/Munich, Germany
hanna.veselovska@tum.de

***Abstract*—In this paper, we propose 1-bit weighted $\Sigma\Delta$ quantization schemes of mixed order as a technique for digital halftoning. These schemes combine weighted $\Sigma\Delta$ schemes of different orders for two-dimensional signals so one can profit both from the better stability properties of low order schemes and the better accuracy properties of higher order schemes. We demonstrate that the resulting mixed-order $\Sigma\Delta$ schemes in combination with a padding strategy yield improved representation quality in digital halftoning as measured in the Feature Similarity Index.**

These empirical results are complemented by mathematical error bounds for the model of two-dimensional bandlimited signals as motivated by a mathematical model of human visual perception.

Key words: digital halftoning, error diffusion, 1-bit quantization, weighted Sigma-Delta

I. Motivation and Previous Works

Digital halftoning is an image reproduction technique that simulates continuous-tone imagery using binary pixel values. That is, for each pixel, each RGB channel can either be active at full intensity or inactive in that location. The human visual system is then smoothing out the sharp changes in the color channel, so that ideally the halftoned image is perceived as similar to the original.

An example is given in Figure 1: the picture on the left is an RGB image while its three counterparts on the right are composed of binary pixels in each of the R, G, and B components, arranged to visually resemble the former as a continuous range RGB image. The key observation that makes this possible is the fact that the human eye can be modeled as a low-pass filter when perceiving visual information from a sufficient distance, blending fine details and recording the average intensity.

There are various competitve methods for digital halftoning such as approaches based on optimization [12], approaches based on neural network design [15, 5], and error diffusion techniques [3, 7, 6, 14, 11] that apply a reccurence relation to compute the halftoned representation.

The latter are often preferred in practice as they are simpler to implement yet competitive in terms of performance; error diffusion will also be the method of choice in this paper. Recently, in [8, 10], the performance of error diffusion techniques has been theoretically analyzed from the perspective of classical 1-bit $\Sigma\Delta$ quantization [1, 4]. It has been shown that weighted higher-order $\Sigma\Delta$ schemes produce halftoned images with higher similarity to the originals [8].

At the same time, the applicability of results available in the $\Sigma\Delta$ literature is limited. Namely, while it has been shown that $\Sigma\Delta$ quantization can be designed to exhibit exponential error decay [2], these results require a significantly smaller amplitude than what is used in the quantized representation. In image representation, these results would hence only be applicable if the intensities all lie close to the average intensity and no very light or very dark spots are present, which is too much of a restriction to be of interest in practice. As shown in [9], this limitation is inherent in the representation and cannot be overcome by an improved quantization scheme.

To address this, a minimal re-scaling of the image has been shown to allow the application of second order schemes with feedback filters that are very spread out and consequently allow for somewhat larger intensities [8]. Due to the very spread-out nature of these filters, however, one needs an initialization strategy: to represent pixels near the upper and left boundary one needs values outside of the image, which need to be set appropriately. In this note, we explore a number of initialization strategies and how they best combine with $\Sigma\Delta$ modulation.

We find that the best performance is observed for an initialization based on mirror images of the image under consideration combined with a mixed order $\Sigma\Delta$ scheme that combines a second and a third order component. The advantage of this scheme is due to its adaption to the smoothness of the initialization – for other strategies such as zero initialization or random initialization, it does not lead to a comparable gain.

The authors acknowledge support by the German Science Foundation (DFG) in the context of the collaborative research center TR-109 and the Emmy Noether junior research group KR 4512/1-1 as well as by the Munich Data Science Institute and Munich Center for Machine Learning. FK would like to thank Sinan Güntürk for pointing out the connection between digital halftoning and $\Sigma\Delta$ quantization; furthermore the authors would like to thank Rongrong Wang for inspiring discussions related to the topic of this paper.

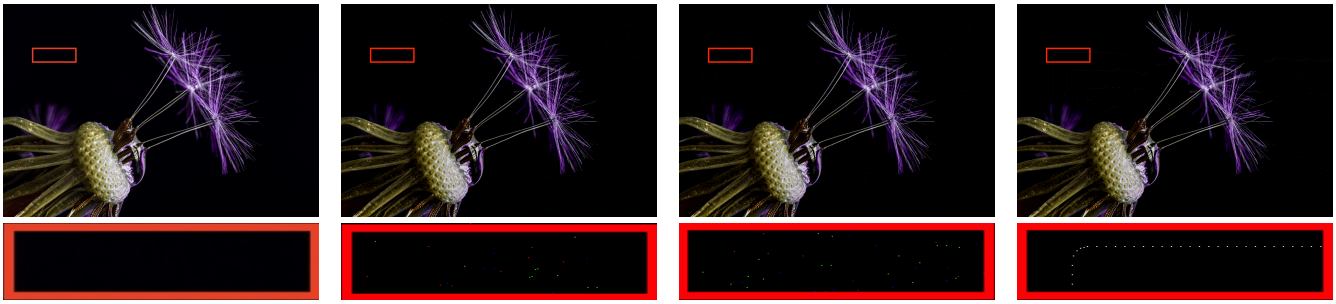

Fig. 1: Digital halftoning using weighted $\Sigma\Delta$ scheme of mixed 3rd and 2nd order with different initial states.
From left to right: ground truth — halftoned with padding — random initial state — zero initial state.
To compare the details, we add zooms of the boxed sections.

120	60	100	120	250	105	107
100	30	30	60	90	100	30
60	30	30	60	90	100	30
120	100	100	120	250	105	107
180	120	120	180	150	150	140
150	33	33	150	150	20	30

TABLE I: *The diagram shows the pattern of symmetric padding of the pixels outside the original image. The pixels of the original image are marked in green and the padded pixels are in blue, and the axes of the image edges are denoted by bold lines.*

II. Image Models, Quantization and Digital Halftoning

In this section, we introduce the problem and model setting following the notation and assumptions from [8], and relying on the key observation that human visual perception involves a smoothing step that can be modeled as a low-pass filter. This characteristic of the human eye makes the class of bandlimited functions of two variables suitable for modelling visual perception.

More precisely, we assume that a visually perceived image can be (at least approximately) represented by a function from the class of functions $\mathcal{B}_{S_\Omega}$ bandlimited to a square $S_\Omega := [-\frac{\Omega}{2}, \frac{\Omega}{2}] \times [-\frac{\Omega}{2}, \frac{\Omega}{2}] \subset \mathbb{R}^2$ in the frequency domain for $\Omega > 0$ large enough. Without loss of generality, we will normalize $\Omega = 1$ for the remainder of this paper. Moreover, for halftoning or quantization, we need is not only bandlimitedness of signals but also boundedness, which motivates the definition of the following class of bandlimited functions with bounded amplitude

$$\mathcal{B}^\mu := \{f \in \mathcal{B}_{S_1} : \ \|f\|_\infty \leq \mu\} \quad \text{for some} \quad \mu > 0. \tag{II.1}$$

Consequently, the process of visual perception can be modeled as a low-pass filter applied to the image of the continuous scene (or a pixeled representation).

Due to the Shannon sampling theorem [13], a low-pass-filter applied to samples of a bandlimited function $f \in \mathcal{B}^\mu$ on the lattice $\mathcal{L} := \frac{1}{\lambda}\mathbb{Z}^2 \subset \mathbb{R}^2$ with an oversampling rate $\lambda > 1$ returns the function, that is,

$$f(\boldsymbol{x}) = \frac{1}{\lambda^2} \sum_{\boldsymbol{n} \in \mathbb{Z}^2} f\big(\tfrac{\boldsymbol{n}}{\lambda}\big)\Phi\big(\boldsymbol{x} - \tfrac{\boldsymbol{n}}{\lambda}\big), \tag{II.2}$$

where the kernel Φ is a Schwartz function with the low-pass property $\mathcal{F}\Phi(\boldsymbol{\xi}) = 1$, if $\boldsymbol{\xi} \in S_\lambda$ and $\mathcal{F}\Phi(\boldsymbol{\xi}) = 0$, if $\boldsymbol{\xi} \notin S_\lambda$.

The goal of digital halftoning of RBG images is to find binary pixels in each of the R, G, and B components whose low-pass representation approximates this signal. That is, fixing the quantization alphabet to be $\mathcal{A} = \{-1, 1\}$, we aim to find a sequence $q_{\boldsymbol{n}} \in \mathcal{A}$, $\boldsymbol{n} \in \mathbb{N}^2$ such that $f \in \mathcal{B}^\mu$ is approximated by

$$f_q(\boldsymbol{x}) = \frac{1}{\lambda^2} \sum_{\boldsymbol{n} \in \mathbb{N}^2} q_{\boldsymbol{n}} \Phi\big(\boldsymbol{x} - \tfrac{\boldsymbol{n}}{\lambda}\big), \qquad \boldsymbol{x} \in \mathbb{R}^2_+. \tag{II.3}$$

We will call the function f_q *a 1-bit representative* of the original function f, and the array $q = \{q_{\boldsymbol{n}}\}_{\boldsymbol{n} \in \mathbb{N}^2}$ is referred to as a *1-bit sample sequence* of f. We aim to construct a 1-bit sequence $\{q_{\boldsymbol{n}}\}_{\boldsymbol{n} \in \mathbb{N}^2}$ in such that, in a suitable sense, $f_q \to f$, $\lambda \to \infty$. We focus, in our mathematical analysis, on the infinity error metric $\|e\|_{L^\infty(\mathbb{R}^2_+)}$, where e is the error signal (or error function) given by $e(\boldsymbol{x}) := f(\boldsymbol{x}) - f_q(\boldsymbol{x})$, $\boldsymbol{x} \in \mathbb{R}^2_+$.

As indicated in [4, 8], introducing the auxiliary function

$$f_\lambda(\boldsymbol{x}) = \frac{1}{\lambda^2} \sum_{\boldsymbol{n} \in \mathbb{N}^2} f\big(\tfrac{\boldsymbol{n}}{\lambda}\big)\Phi\big(\boldsymbol{x} - \tfrac{\boldsymbol{n}}{\lambda}\big), \qquad \boldsymbol{x} \in \mathbb{R}^2_+, \tag{II.4}$$

the error signal e can be decomposed into the sum of two error therms $e = e_f + e_q$ such that

$$e_f(\boldsymbol{x}) := f(\boldsymbol{x}) - f_\lambda(\boldsymbol{x}), \quad e_q(\boldsymbol{x}) := f_\lambda(\boldsymbol{x}) - f_q(\boldsymbol{x}). \tag{II.5}$$

Since the first term e_f is independent of the quantization process, it is natural to focus on the second term e_q, which will be referred to as *quantization error*. At the same time, e_f is of relevance and can lead to artifacts, especially near the boundary. See Fig 1 for the illustration of one of the typical artifacts.

One of the main goals of this paper is to reduce this effect by considering suitable initialization strategies. To mitigate the boundary artifacts, we propose to use *symmetric image padding* [16]. Namely, given an image of a particular size, we

Weight matrix $\mathbf{W}_2$	(i,j)-Index sets	Filters $h^2_{i,j}$	Weight matrix $\mathbf{W}_3$	(i,j)-Index sets	Filters $h^3_{i,j}$
$\begin{pmatrix} 0 & \mathbf{0} & \frac{82}{199} & \frac{6}{199} \\ \frac{12}{199} & \frac{82}{199} & \frac{1}{199} & 0 \\ 0 & \frac{5}{199} & 0 & 0 \end{pmatrix}$	$(0,1),(1,j),\ j\in\{-1,0,1\}$	$h^2_{i,j}=h^2_{540},\ h^2_{i,j}=h^2_{580}$	$\begin{pmatrix} 0 & \mathbf{0} & \frac{6}{199} \\ 0 & \frac{5}{199} & 0 \end{pmatrix}$	$(0,1),(1,0)$	$h^3_{i,j}=h^3_{390}$
	$(2,0),(0,2)$	$h^2_{i,j}=h^2_3$			

TABLE II: *Weighted $\Sigma\Delta$ schemes of mixed 2nd and 3rd order used for for digital halftoning in Sec. IV. The element $w_{0,0}$ is denoted in bold.*

pad the edges of the image with extra pixels such that the added pixels mirror the edge of the image, see the diagram in Table I. The padded pixels are used only for the internal calculation of 1-bit pixels where the corresponding padding size will be determined by the type weighted $\Sigma\Delta$ schemes used in the halftoning process. The padded pixels and the true image will then be considered as a single image input to the halftoning algorithm. The halftoned output image will have the same dimensions as the original RGB image by cutting the padded pixels at the output, however, we believe that the image padding procedure will allow to eliminate the contribution of e_f to quantization error due to a smooth transition at the edges of the true image.

III. Weighted $\Sigma\Delta$ Schemes of Mixed Orders

In this section, we will introduce the weighted $\Sigma\Delta$ schemes of mixed orders with symmetric padding. We begin with recalling some important concepts related to directional convolutions in two dimensions, and feedback filters, following the notation in [4, 8].

For a positive integer r and a sequence $g \in \ell^1$ with $g_n = 0$ for $n < 0$, the *feedback filter* h is called *of order* r as soon as h satisfies the identity $\delta^0 - h = \Delta^r g$, where δ^a denotes the Kronecker delta sequence situated at the integer a, and Δ is the backward difference sequence given by $\Delta_0 = 1$, $\Delta_1 = -1$, $\Delta_k = 0$, for all $k \in \mathbb{Z} \setminus \{0,1\}$. We define the filter constant for the rth-order filter h as

$$C_h := \sum_{j=1}^{L} h_j j^r. \tag{III.1}$$

Definition III.1. Given a feedback filter $h = \{h_j\}_{j\in\mathbb{Z}}$ with its support on the first L elements and a two-index sequence $v = \{v_{\boldsymbol{n}}\}_{\boldsymbol{n}\in\mathbb{Z}^2}$, we denote by $h *_{\mathbf{d}} v$ the convolution of v and h in the direction $\mathbf{d} = (d_1, d_2) \in \mathcal{L}$ and define it as

$$(h *_{\mathbf{d}} v)_{\boldsymbol{n}} = \sum_{j=1}^{L} h_j v_{\boldsymbol{n}-j\mathbf{d}} \tag{III.2}$$

Besides, let us denote by $y_{\boldsymbol{n}} := f(\frac{\boldsymbol{n}}{\lambda})$, $\boldsymbol{n} \in \mathbb{N}^2$ the elements of sample sequence y with the oversampling rate $\lambda > 1$ of a function $f \in \mathcal{B}^\mu$. Additionally, consider some set of orders $\Xi := \{r_1, \ldots, r_N\}$ with $r_j \geq 1$ for all $j = 1, \ldots, N$. For each $r \in \Xi$, we will fix a batch of direction sets $\mathbf{d}^r_{i,j}$ with $i \in \{0, \ldots, p_r\}$ and $j \in \{-s_r, \ldots, \ell_r\}$ for some $\ell_r, s_r, p_r \in \mathbb{N}$. For these $\ell_r, s_r, p_r \in \mathbb{N}$, we average all $\Sigma\Delta$ schemes of order r along these directions with the *weight matrix* $\mathbf{W}_r \in \mathbb{R}^{(\ell_r+s_r+1)\times(p_r+1)}$ given by

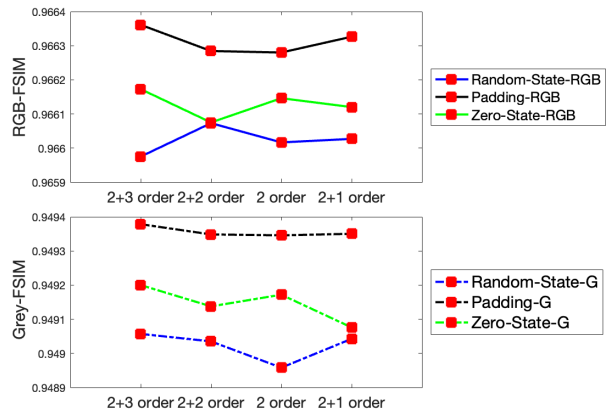

Fig. 2: *Averaged FSIM over 50 images and their halftoned counterparts generated by different weighted $\Sigma\Delta$ schemes.*

$$\mathbf{W}_r = \begin{pmatrix} 0 & \cdots & 0 & w^r_{0,1} & \cdots & w^r_{0,\ell} \\ w^r_{1,-s} & \cdots & w^r_{1,0} & w^r_{1,1} & \cdots & w^r_{1,\ell} \\ \vdots & \ddots & \vdots & \vdots & \ddots & \vdots \\ w^r_{p,-s} & \cdots & w^r_{p,0} & w^r_{p,1} & \cdots & w^r_{p,\ell} \end{pmatrix}, \tag{III.3}$$

such that $\sum_{i=0}^{p} \sum_{j=-s}^{\ell} w^r_{i,j} = 1$. For the global average over different orders from Ξ, we will use the weight $\theta_{r_1}, \ldots, \theta_{r_N}$ and assume that $\theta_{r_j} \geq 0$ and

$$\theta_{r_1} + \ldots + \theta_{r_N} = 1. \tag{III.4}$$

Now, we will now introduce weighted $\Sigma\Delta$ quantization schemes of mixed orders.

Definition III.2. For a given sample sequence $y = \{y_{\boldsymbol{n}}\}_{\boldsymbol{n}\in\mathbb{N}^2}$, the *weighted $\Sigma\Delta$-quantizer of mixed order* with the weight matrices $\mathbf{W}_r$ and global weights $\theta_{r_1}, \ldots, \theta_{r_N}$ is given by

$$v_{\boldsymbol{n}} - \sum_{r\in\Xi} \theta_r \sum_{i\,j} w^r_{i,j} \big(h^r_{i,j} *_{\mathbf{d}^r_{i,j}} v\big)_{\boldsymbol{n}} = y_{\boldsymbol{n}} - q_{\boldsymbol{n}} \tag{III.5}$$

$$q_{\boldsymbol{n}} = \operatorname{sign}\Big(\sum_{r\in\Xi} \theta_r \sum_{i\,j} w^r_{i,j} \big(h^r_{i,j} *_{\mathbf{d}^r_{i,j}} v\big)_{\boldsymbol{n}} + y_{\boldsymbol{n}}\Big), \tag{III.6}$$

where, for each order $r \in \Xi$, single-index filter $h^r_{i,j} = \left\{(h^r_{i,j})_n\right\}_{n\in\mathbb{Z}} \in \ell^1(\mathbb{Z})$ is a feedback filter of order r, e.i. it fulfills the condition $\delta^0 - h^r_{i,j} = \Delta^r g^r_{i,j}$ for sequences $g^r_{i,j} \in \ell_1(\mathbb{Z})$ with $g^r_{i,jn} = 0$ for $n < 0$.

Corollary III.1. *Consider a bandlimited function $f \in \mathcal{B}^\mu$ sampled on the lattice $\frac{1}{\lambda}\mathbb{N}^2$ with $\lambda > 1$. If we use a weighted $\Sigma\Delta$ scheme* (III.5)-(III.6) *for construction of f's 1-bit samples $q \in \{-1,1\}^{\mathbb{N}^2}$, then the corresponding quantized representative f_q satisfies*

$$\|f_\lambda - f_q\|_\infty \le \|v\|_\infty \Big(\sum_{r\in\Xi} \frac{\theta_r}{\lambda^r} \left(C_{\mathbf{W}_r} \cdot C \cdot \|\nabla^r \Phi\|_{1,2} + \mathcal{O}(\lambda^{-1}) \right) \Big),$$

where $C > 0$ is a constant independent of $\mathbf{W}_r$, Φ is a Schwartz function of the suitable low-pass type, and

$$(C_{\mathbf{W}_r})^2 := \sum_{m=0}^{r} \Big(\sum_{i=0}^{p_r} \sum_{j=-s_r}^{\ell_r} w^r_{i,j} \cdot C_{h^r_{i,j}} \cdot i^{r-m} j^m \Big)^2, \quad \text{(III.7)}$$

are weight constants of order r with filter constants $C_{h^r_{i,j}}$ as in (III.1)*, and* $(\|\nabla^r \Phi\|_{1,2})^2 := \sum_{|\alpha|=r} \frac{1}{\alpha!} \|\partial^\alpha \Phi\|_1^2$.

Proof of Cor III.1. Using the definition of scheme (III.5)-(III.6) and the error term e_q in (II.5) we can represent $e_q(\boldsymbol{x})$ as

$$f_\lambda(\boldsymbol{x}) - f_q(\boldsymbol{x}) = \sum_{r\in\Xi} \theta_r \big(\tfrac{1}{\lambda^2} \sum_{\boldsymbol{n}\in\mathbb{N}^2} v_{\boldsymbol{n}} \big(\Phi\left(\boldsymbol{x} - \frac{\boldsymbol{n}}{\lambda}\right) - \sum_{i\,j} w^r_{i,j} \sum_{s=1}^{L} (h^r_{i,j})_s \Phi\Big(\boldsymbol{x} - \tfrac{\boldsymbol{n} + s\mathbf{d}^r_{i,j}}{\lambda}\big)\big)\big)$$

since all θ_r sum up to one. Bounding the factors near each θ_r as in [8] for weighted $\Sigma\Delta$ schemes of order r, gives the stated result. □

As the weighted $\Sigma\Delta$ schemes [8], the mixed order schemes (III.5)-(III.6) enjoy stability, i.e. the accumulated error recorded in v is bounded, with $\|v\|_\infty \le 1$, if the sample sequence y and the involved feedback filters have not too large norms, in the sense $\sum_{r\in\Xi} \theta_r \sum_{i\,j} w^r_{i,j} \left\|h^r_{i,j}\right\|_1 + \|y\|_\infty \le 2$.

We propose to use mixed order $\Sigma\Delta$ schemes together with symmetric padding described in Sec. II for the digital halftoning of images. This combination, on the one hand, can benefit from a good balance between the stability of lower-order feedback filters and a better halftoning performance furnished by higher-order filters. On the other hand, the padding strategy of the correct size allows for mitigating the halftoning boundary artifacts. The size of the padding process can be determined as follows. Suppose that all feedback filters $h^r_{i,j}$ used in the mixed order scheme (III.5)-(III.6) are supported on at most the first $L \in \mathbb{N}$ entries. Then, to have all filter elements active in (III.5)-(III.6) when quantizing the first samples of $y_{\boldsymbol{n}}$, we pad the image symmetrically as illustrated in Tab I with L extra pixels, initialize the state variable v to zero, and then we use this extended image for obtaining the halftone representative of the original.

IV. Mixed Order Schemes in Numerical Practice for Halftoning

In this section, we illustrate that the usage of mixed order weighted $\Sigma\Delta$ schemes for digital halftoning leads to a higher visual similarity between the halftoned image and the original measured by the state-of-the-art Feature Similarity Index (FSIM) [17].

We explain our setup for color images, gray-scale images are treated analogously. We represent color images as RGB matrices, $\mathcal{I}_{RGB} := \left\{\mathcal{I}^{RGB}_{n_1,n_2}\right\}^{N_1,N_2}_{n_1,n_2=0}$, consisting of three color channels, each given as a sample array. In order to construct a halftoned counterpart of $\mathcal{I}_{RGB}$, we use Algorithm 1.

Here, we will work with the family of second-order and third-order feedback filters with minimal support given by

$$h^2_\kappa = [0,\, (h^2_\kappa)_1, \ldots, 0,\, (h^2_\kappa)_{\kappa+1}], \quad \text{(IV.1)}$$

with non-zero elements $(h^2_\kappa)_1 = \frac{\kappa+1}{\kappa}$, $(h^2_\kappa)_{\kappa+1} = -\frac{1}{\kappa}$, and

$$h^3_\kappa = [0,\, (h^3_\kappa)_1, \ldots, 0,\, (h^3_\kappa)_{\kappa+1}, \ldots, 0,\, (h^3_\kappa)_{2\kappa+1}], \quad \text{(IV.2)}$$

with $(h^3_\kappa)_1 = \frac{2\kappa^2+3\kappa+1}{2\kappa^2}$, $(h^3_\kappa)_{\kappa+1} = -\frac{2\kappa+1}{\kappa^2}$, $(h^3_\kappa)_{2\kappa+1} = \frac{\kappa+1}{2\kappa^2}$, respectively. The norms of such filters differ only slightly as $\left\|h^2_\kappa\right\|_1 = 1 + \frac{2}{\kappa}$ and $\left\|h^2_\kappa\right\|_1 = 1 + \frac{4}{\kappa} + \frac{2}{\kappa^2}$.

Algorithm 1: Digital Halftoning of Images with Weighted $\Sigma\Delta$ Schemes of Mixed Orders and Padding

Data:
- RGB image $\mathcal{I}_{RGB} := \left\{\mathcal{I}^{RGB}_{n_1,n_2}\right\}^{N_1,N_2}_{n_1,n_2=0} \in [-1,1]^{N_1\times N_2\times 3}$

Quantization setup:
- Define: $\Sigma\Delta$ orders $\Xi = \{r_1, \ldots, r_N\}$, weight matrices $\mathbf{W}_r$ directions $\mathbf{d}^r_{i,j}$, feedback filters $h^r_{i,j}$

begin

Padding $\mathcal{I} = 0.999 \cdot \text{padding}(\mathcal{I}, L)$
for $c = R, G, B$ and $\boldsymbol{n} = (n_1, n_2)$ with
$n_1 = 1, ..., N_1 + L$
$n_2 = 1, ..., N_2 + L$

$$v^c_{\boldsymbol{n}} - \sum_{r\in\Xi} \theta_r \sum_{i\,j} w^r_{i,j} \big(h^r_{i,j} *_{\mathbf{d}^r_{i,j}} v^c\big)_{\boldsymbol{n}} = \mathcal{I}^c_{\boldsymbol{n}} - q^c_{\boldsymbol{n}}$$

$$q^c_{\boldsymbol{n}} = \text{sign}\big(\sum_{r\in\Xi} \theta_r \sum_{i\,j} w^r_{i,j} \big(h^r_{i,j} *_{\mathbf{d}^r_{i,j}} v^c\big)_{\boldsymbol{n}} + \mathcal{I}^c_{\boldsymbol{n}} \big)$$

Result:
- 1-bit image $q = \left\{q^c_{n_1,n_2}\right\}^{N_1,N_2}_{n_1,n_2=L} \in \{-1,1\}^{N_1\times N_2\times 3}$
- *bmp*-image $\mathcal{I}_q \in \{0,255\}^{N_1\times N_2\times 3}$
- halftoning error $FSIM(\mathcal{I}, \mathcal{I}_q)$

In our numerical experiments, we use 50 distinct color images of the size 1920×1280 and their gray-scale counterparts. We compare four different weighted $\Sigma\Delta$ of mixed orders with three different initialization strategies. Namely, the setting for the weighted $\Sigma\Delta$ of $2+3$ order is described in Table II, with weight matrices chosen to allow stability with minimal image re-scaling. For the weighted $\Sigma\Delta$ of $2+1$ order, we use the weight matrices and 2nd-order filters as Table II, and we set $W_1 := W_3$ with the 1st-order filter. The weighted $\Sigma\Delta$ of $2+2$ is built as the $3+2$ scheme with h^3_{390} substituted by h^2_{390}. The scheme under the name "2 order" in Fig 2 is set as in

[8]. To measure the quality of the resulting halftoned images, we compute the FSIM [17] for each image and its halftoned version, and the more similar these images are, the higher the corresponding FSIM is.

As it can be seen in Def. (III.5)-(III.6), the initialization of the state variable v plays a key role in how active the feedback filters are when quantizing pixels close to the image boundary. If v is initialized as zero, see "Zero-State" in Fig 2, and used with spread-out filters of higher orders, this leads to a good performance only in image regions with all filters active and may cause artifacts near boundary regions with almost constant amplitude. To avoid such a problem, in [8] v was initialized randomly, see "Random-state" in Fig 2. Here, we propose to use symmetric padding as described in Sec II and III, which is indicated accordingly in Fig 2 starting the zero state.

The results of numerical experiments are summarized in Figure 2 as the average FSIM over 50 images for different weighted $\Sigma\Delta$ halftoning techniques. Even though random initialization eliminates boundary artifacts, it reduces the similarity between images in general. The best performance in this quality measure is achieved by the newly proposed mixed order weighted $\Sigma\Delta$ schemes with second-order and third-order building blocks as in Table II combined with padding.

References

[1] Ingrid Daubechies and Ron DeVore. "Approximating a bandlimited function using very coarsely quantized data: A family of stable sigma-delta modulators of arbitrary order". In: *Annals of mathematics* 158.2 (2003), pp. 679–710.

[2] Percy Deift, Felix Krahmer, and C Sınan Güntürk. "An optimal family of exponentially accurate one-bit Sigma-Delta quantization schemes". In: *Communications on Pure and Applied Mathematics* 64.7 (2011), pp. 883–919.

[3] Steinberg L. Floyd R. "An adaptive algorithm for spatial gray-scale". In: *Proc. Soc. Inf. Disp.* Vol. 17. 1976, pp. 75–77.

[4] C Sinan Güntürk. "One-bit sigma-delta quantization with exponential accuracy". In: *Communications on Pure and Applied Mathematics: A Journal Issued by the Courant Institute of Mathematical Sciences* 56.11 (2003), pp. 1608–1630.

[5] Win-Bin Huang, Alvin WY Su, and Yau-Hwang Kuo. "Neural network based method for image halftoning and inverse halftoning". In: *Expert Systems with Applications* 34.4 (2008), pp. 2491–2501.

[6] John F Jarvis, C Ni Judice, and WH Ninke. "A survey of techniques for the display of continuous tone pictures on bilevel displays". In: *Computer graphics and image processing* 5.1 (1976), pp. 13–40.

[7] Donald E Knuth. "Digital halftones by dot diffusion". In: *ACM Transactions on Graphics (TOG)* 6.4 (1987), pp. 245–273.

[8] Felix Krahmer and Anna Veselovska. "Enhanced Digital Halftoning via Weighted Sigma-Delta Modulation". In: *arXiv preprint arXiv:2202.04986* (2022).

[9] Felix Krahmer and Rachel Ward. "Lower bounds for the error decay incurred by coarse quantization schemes". In: *Applied and Computational Harmonic Analysis* 32.1 (2012), pp. 131–138.

[10] He Lyu and Rongrong Wang. "Sigma Delta quantization for images". In: *arXiv preprint arXiv:2005.08487* (2020).

[11] Victor Ostromoukhov. "A simple and efficient error-diffusion algorithm". In: *Proceedings of the 28th annual conference on Computer graphics and interactive techniques*. 2001, pp. 567–572.

[12] Wai-Man Pang et al. "Structure-aware halftoning". In: *ACM SIGGRAPH 2008 papers*. 2008, pp. 1–8.

[13] Daniel P Petersen and David Middleton. "Sampling and reconstruction of wave-number-limited functions in N-dimensional Euclidean spaces". In: *Information and control* 5.4 (1962), pp. 279–323.

[14] Jeng-Nan Shiau and Zhigang Fan. "Set of easily implementable coefficients in error diffusion with reduced worm artifacts". In: *Color Imaging: Device-Independent Color, Color Hard Copy, and Graphic Arts*. Vol. 2658. SPIE. 1996, pp. 222–225.

[15] Barry L Shoop and Eugene K Ressler. "An error diffusion neural network for digital image halftoning". In: *Proceedings of 1995 IEEE Workshop on Neural Networks for Signal Processing*. IEEE. 1995, pp. 427–436.

[16] Hongxiang Tang, Alessandro Ortis, and Sebastiano Battiato. "The impact of padding on image classification by using pre-trained convolutional neural networks". In: *Image Analysis and Processing–ICIAP 2019: 20th International Conference, Trento, Italy, September 9–13, 2019, Proceedings, Part II 20*. Springer. 2019, pp. 337–344.

[17] Lin Zhang et al. "FSIM: A feature similarity index for image quality assessment". In: *IEEE transactions on Image Processing* 20.8 (2011), pp. 2378–2386.